UNIVERSITY OF LIEGE
Department *Mécanique des matériaux & Structures*

ELEMENTS OF THEORY FOR SAFIR 2002

A COMPUTER PROGRAM FOR ANALYSIS OF STRUCTURES SUBMITTED TO THE FIRE

by

J.M. Franssen[1], V.K.R Kodur[2], J. Mason[3]

Augustus 2002

[1] Univ. of Liege, Belgium
[2] National Research Council of Canada, Institute For Research In Construction, Ottawa, Canada
[3] Sinclair Knight Merz, Wellington, N. Z.

1 THE TRUSS ELEMENT 3

1.1 GEOMETRY 3
1.2 INTEGRATION ON THE VOLUME 3
1.3 STRAIN 3
1.4 NODAL FORCES 3
1.5 STIFFNESS MATRIX 4

2 THE BEAM ELEMENT 5

Assumptions for beam elements: 5

3 THE SHELL ELEMENT 6

3.1 GEOMETRY 6
3.2 POINTS OF INTEGRATION 6
3.3 REBAR 7
3.4 INFLUENCE OF THE BARS ON THE STIFFNESS OF THE SHELL 7

4 THE SOLID ELEMENT 10

4.1 CONDUCTION [5] 10
4.1.1 Introduction 10
4.1.2 Background 10
4.1.3 General Formulation 10
4.1.4 Weighted Residual Methods 12
4.1.5 Shape Functions 12
4.1.6 Finite Element Formulation in Two Dimensions 14
4.1.7 Triangular (3 node) Elements 16
4.1.8 Rectangular (4 node) Element 20
4.1.9 Convective Boundary Conditions 21
4.1.10 Time-Dependant (Transient) Problems 22
4.1.11 Non-Linear Problems 25
4.1.12 Enthalpy formulation 25
4.2 INTERNAL VOIDS 29
4.2.1 Convection 29
4.2.2 Radiation 30

5 CONVERGENCE CRITERIA 31

6 STORAGE OF STIFFNESS MATRIX 33

7 NOMENCLATURE 34

8 REFERENCES 34

1 The TRUSS Element

1.1 Geometry

The truss element is straight with two end nodes. The geometry is defined by the position of these end nodes. The truss element is completely defined by its cross sectional area and the material type. Only one material, one temperature and one strain is present in each element.

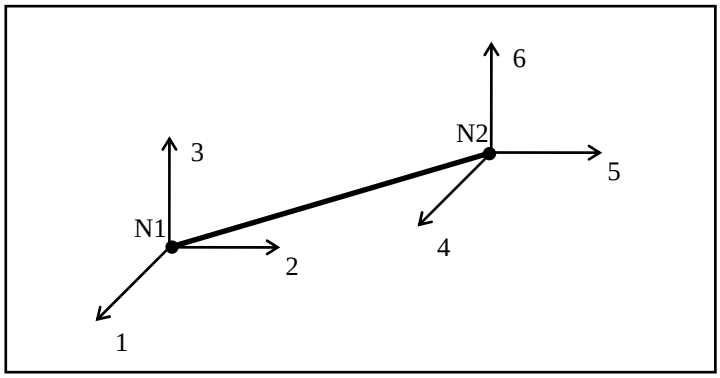

Figure 7: Truss element - Degrees of freedom at nodes

1.2 Integration on the volume

All integrations are made analytically. Hence, no points of integration are given in the program for truss elements.

1.3 Strain

The strain is uniform in the element and calculated according to:

$$\varepsilon = \frac{1}{2}\left(\frac{L^2 - L_0^2}{L_0^2}\right) \qquad (1)$$

where L is the deformed length of the element, and L_0 is the un-deformed length of the element.

1.4 Nodal forces

In the co-rotational configuration, the two longitudinal forces are calculated according to:

$$f_x^{\text{int}} = \pm \text{As}\frac{\text{L}}{\text{L}_\text{o}} \qquad (2)$$

where A is the cross sectional area, and s is the stress.

1.5 Stiffness matrix

With the nodal displacements ordered as:

$$\mathbf{p}^{\mathrm{T}} = \rangle u_1 \quad v_1 \quad w_1 \quad u_2 \quad v_2 \quad w_2 \langle \tag{3}$$

the stiffness matrix has the form:

$$\mathbf{K} = \mathbf{K_u} + \mathbf{K_s} \tag{4}$$

where

$$\mathbf{K_u} = E_t A \frac{L^2}{L_0^3} \begin{bmatrix} 1 & 0 & 0 & -1 & 0 & 0 \\ & 0 & 0 & 0 & 0 & 0 \\ & & 0 & 0 & 0 & 0 \\ & & & 1 & 0 & 0 \\ & \text{SYM} & & & 0 & 0 \\ & & & & & 0 \end{bmatrix} \tag{5}$$

and

$$\mathbf{K}_s = \frac{sA}{L_0} \begin{bmatrix} 1 & 0 & 0 & -1 & 0 & 0 \\ & 1 & 0 & 0 & -1 & 0 \\ & & 1 & 0 & 0 & -1 \\ & & & 1 & 0 & 0 \\ & \text{SYM} & & & 1 & 0 \\ & & & & & 1 \end{bmatrix} \tag{6}$$

with E_t defined by the material model:

$$E_t = \frac{ds}{d\varepsilon} \tag{7}$$

2 *The BEAM Element*

The beam element is straight in its un-deformed geometry. Its position in space is defined by the position of three nodes: the two end nodes (N1-N2), and a third node (N4) defining the position of the local y axis of the beam. The node N3 is used to support an additional degree of freedom.

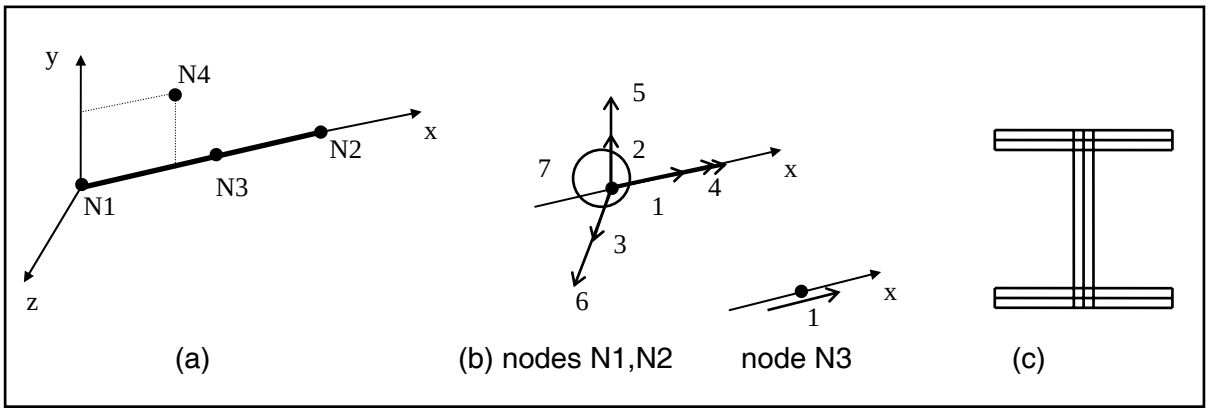

Figure 8: Beam element: (a) Local axes (b) Degrees of freedom at nodes (c) Cross section

To describe the geometry of the cross section, the fibre model is used. The cross section of the beam is subdivided into small fibres (triangles, quadrilaterals or both). The material behaviour of each fibre is calculated at the centre of the fibre and it is constant for the whole fibre. Each fibre has it's own material, this allows for the building of composite sections made of different materials.

Assumptions for beam elements:

- the Bernoulli Hypothesis is considered, i.e., the cross section remains plane under bending moment
- plastifications are only considered in the longitudinal direction of the member, that is uni-axial constitutive models
- non-uniform torsion is considered

3 The SHELL Element

3.1 Geometry

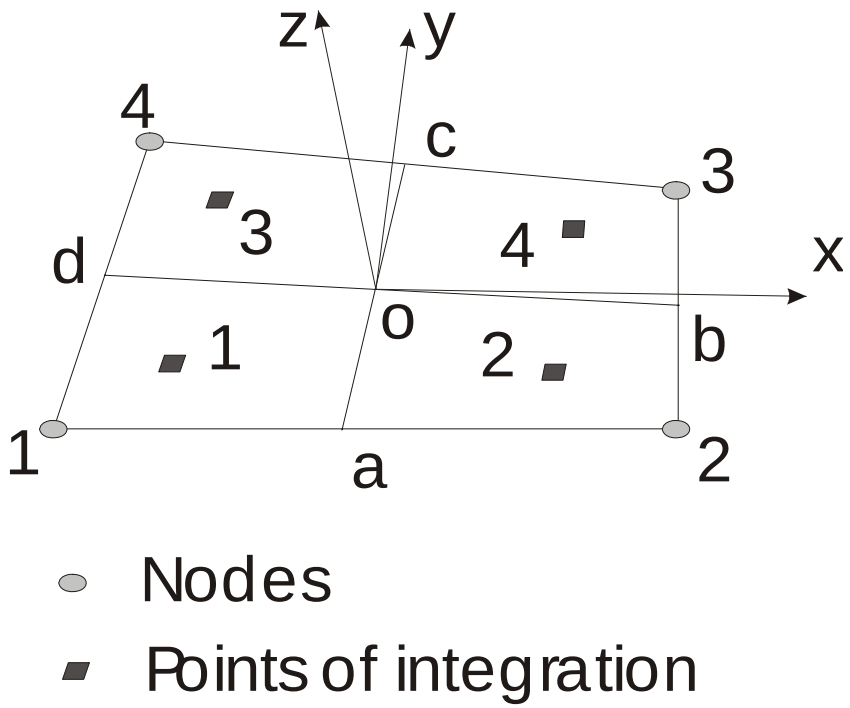

Figure 11-a : Definition of the geometry and local axes

The nodes are in the order 1, 2, 3, 4.
a, b, c, d are the middle points of the edges of the elements.
o, the centre of the local system of co-ordinates is at the intersection between a-c and b-d.
z has the direction of d-b ^ a-c.
x and y are perpendicular to z and their direction is chosen as to have the same angle between o-b and x, on one hand, and o-c and y, on the other hand.
As a particular case, if the element is a plane rectangle, x is the median 0-b and y is the median o-c.

3.2 Points of integration

There are 4 points of integration on the surface of the element, see Figure 11 a. In each direction, the integration is by the method of gauss.
The number of integration points on the thickness is chosen by the user, from 2 to 10. The integration is also by the method of Gauss.

3.3 Rebar

Different layers of rebars can be present in the element. The rebar layers are horizontal (i.e. parallel to the local **x, y** plane). The rebars are uniformly distributed (layered rebars). Each layer is defined by:

- it's local vertical coordinate **z** in the element (this level must not necessarily coincide neither with the position of a point of integration on the thickness, nor with a position where the temperature has been calculated. Linear interpolations are made);
- it's cross section per unit length of width (m^2/m for example);
- it's material number; and
- the angle between the direction of the rebars and the local **x** axis..

Assumptions for rebar elements are:

- the cross section of the rebar is not subtracted from the plane section of the element. This means that, in a reinforced concrete slab, steel and concrete are supposed to be simultaneously present at the location of the bars,
- the bars resist only axial direction actions. This means that a mesh of perpendicular rebars does not resist shear by itself.

The figure 11-b is made for a rectangular element, and shows the way in which the angle is measured.

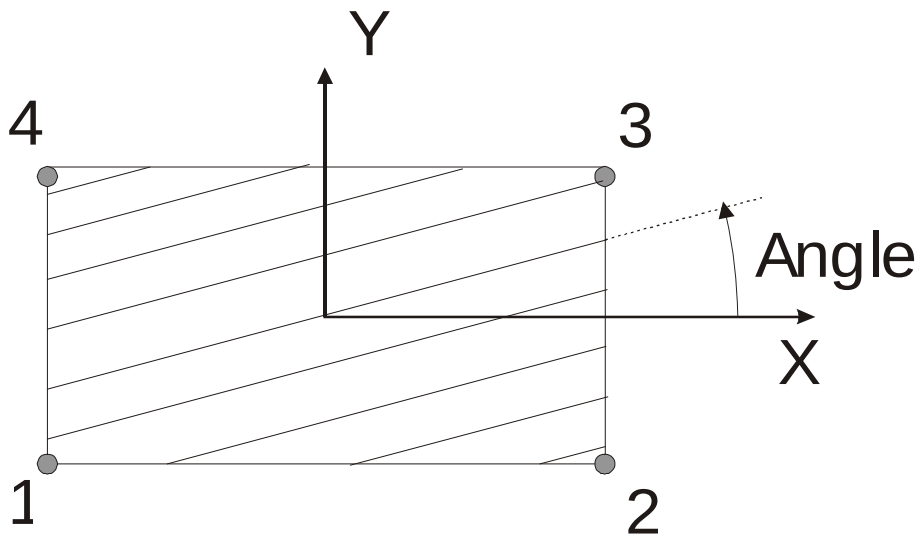

Figure 11: Definition of the variable '*angle*'

The angle will be called θ in the later development:

3.4 Influence of the bars on the stiffness of the shell

A strain state $\left(\varepsilon_x, \varepsilon_y, \varepsilon_{xy}\right)$ in the shell, will generate a strain in the bars which is calculated by equation 1. Figure 12 shows how the component generated by ε_x is derived.

$$\varepsilon_{bar} = \left|\cos(\theta)\right|\varepsilon_x + \left|\sin(\theta)\right|\varepsilon_y \quad (1)$$

The absolute values are taken in order to obtain "tension leads to tension", even if the angle is higher than 90° or is smaller than 0°.

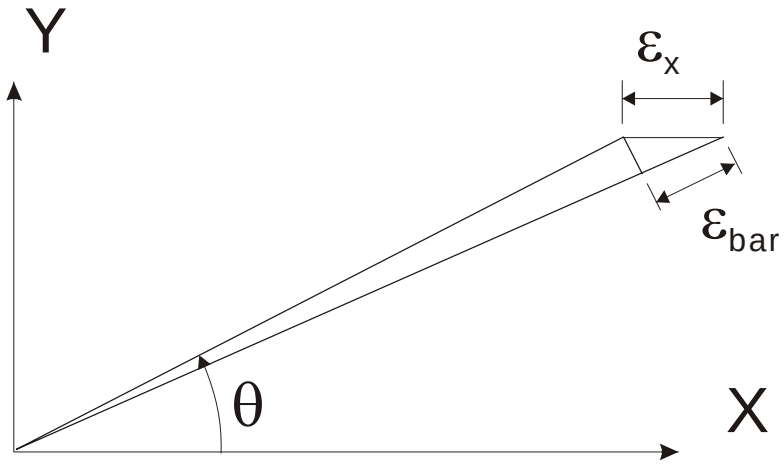

Figure 12: relationship between the strains

The uniaxial material law in the bars can be expressed by equation 2 (with a secant modulus) or equation 3 (with a tangent modulus).

$$\sigma_{bar} = E_{\sec}\,\varepsilon_{bar} \quad (2)$$

$$d\sigma_{bar} = E_t\,d\varepsilon_{bar} \quad (3)$$

A stress σ_{bar} in the bars (in N/m²) will generate a stress state in the shell (in N/m) which is calculated by equation 4. Figure 13 shows how the components are generated.

$$\sigma_{shell} = \left(\sigma_x;\sigma_y;\sigma_{xy}\right) = A_{bar}\,\sigma_{bar}\left(\left|\cos(\theta)\right|;\left|\sin(\theta)\right|;0\right) \quad (4)$$

This stress has to be integrated on the width of the element in order to evaluate the equivalent nodal forces.

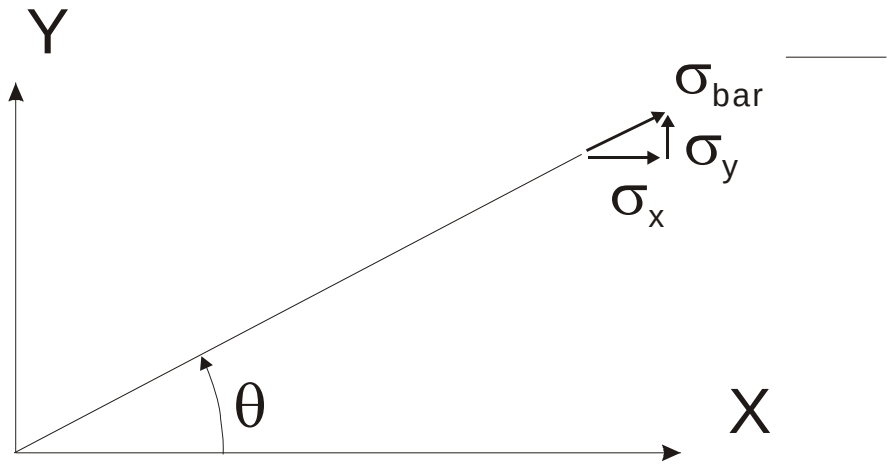

Figure 13: relationship between the stresses

Combining equations 1, 2 and 4, for example, yields equation 5 which gives the increase of stiffness of the shell provided by the presence of the bars. Simply note that the equivalent relation with tangent modulus and increment of stresses and strains is in fact used in the code.

$$\begin{pmatrix} \sigma_x \\ \sigma_y \end{pmatrix} = A_{bar}\, E_s \begin{pmatrix} \left|\cos^2(\theta)\right| & \left|\cos(\theta)\sin(\theta)\right| \\ \left|\cos(\theta)\sin(\theta)\right| & \left|\sin^2(\theta)\right| \end{pmatrix} \begin{pmatrix} \varepsilon_x \\ \varepsilon_y \end{pmatrix} \qquad (5)$$

4 The SOLID Element

4.1 Conduction [5]

4.1.1 Introduction

This section reviews the finite element method for heat transfer analysis, describing the principles of the finite element method and the derivation of the matrix form of the heat transfer equations. The derivation of the element stiffness matrices for two simple element types used in SAFIR is explained. The chapter concludes with a brief discussion of non-linear and time-dependant finite element analysis. Only two-dimensional analysis is discussed here, three-dimensional analysis is a relatively straightforward extension of the theory for two dimensions.

The material in this chapter results from a review of a number of references, see [6], [7] and [8].

4.1.2 Background

The Finite Element Method is a numerical method for analysing continuous domains. Exact solutions of the governing equations for most practical problems can only be obtained for simple problems or problems in which restrictive assumptions are made with respect to geometry, material properties, and/or boundary conditions. Numerical solution methods are needed for the analysis of practical problems. The finite element method is commonly used for problems that are too complicated to be solved by classical analytical methods.

The Finite Element Method views a domain as an assembly of simple geometric shapes (called finite elements). The method is based on the concept that the solution of a differential equation can be reformulated as a linear combination of a series of unknown parameters and appropriately selected functions (called approximation functions or interpolation functions). The approximation functions are selected so that they satisfy the boundary conditions. Real problems are often based on geometric complex regions, and it is difficult to select approximation functions that satisfy the boundary conditions. If the region can be represented as a series of simple subdomains (or finite elements) that permit of the generation of approximation functions that satisfy the boundary conditions of each element, then the problem should be able to be solved.

4.1.3 General Formulation

The general equation for two-dimensional heat conduction in an isotropic material is

$$\left(k\frac{\partial^2 T}{\partial x^2} + k\frac{\partial^2 T}{\partial y^2} \right) + Q = \rho c \frac{\partial T}{\partial t} \qquad (3.1a)$$

or

$$k\nabla^2 T + Q = \rho c \frac{\partial T}{\partial t} \qquad (3.1b)$$

where k is the thermal conductivity of the material, T is the temperature, Q is the amount heat generated in the material per unit volume, ρ is the density, c is the heat capacity, and t is time.

If steady-state conditions exist, i.e. the temperature does not change with time, then the equation reduces to

$$k\nabla^2 T + Q = 0 \tag{3.2}$$

If there is no internal heat generation then the equation further reduces to

$$k\nabla^2 T = 0 \tag{3.3}$$

The boundary conditions may be a known temperature and/or a known heat flux (both conditions may not be specified over the same part of the boundary).

Known temperature

The temperature may be specified, i.e. $T=T_O$

Known Heat flux

The heat flow may be specified. This requires that

$$q = -k\frac{\partial T}{\partial n} \tag{3.4a}$$

or

$$k\frac{\partial T}{\partial n} + q = 0 \tag{3.4b}$$

where q is the specified heat flow, and n is the outward normal vector to the boundary.

This can be written in the alternative form

$$k\left(\frac{\partial T}{\partial x}n_x + \frac{\partial T}{\partial y}n_y\right) + q = 0 \tag{3.4c}$$

where nx and ny are the components of the outward normal vector parallel to the x and y axes.

For the heat transfer problem to be defined, at least one of these conditions must be specified on at least part of the boundary.

This classical formulation (equation 3.1b) is suitable for solution by the finite difference method, but must be replaced by a variational formulation for Finite Element Analysis. A weighted residual method is normally used for this.

4.1.4 Weighted Residual Methods

Several methods can be used to transform the heat transfer equation to a form suitable for Finite Element Analysis. The most common is the Weighted Residual Method.

Consider a general differential equation of the form

$$a\frac{\partial^2 u}{\partial x^2} + b = 0 \tag{3.5}$$

The solution of this equation, u, can be approximated by a function

$$\bar{u}(x) = a_1\phi_1(x) + a_2\phi_2(x) + ... + a_n\phi_n(x)$$

or

$$\bar{u}(x) = \sum_{i=1}^{n} a_i\phi_i(x) \tag{3.6}$$

$\bar{u}$ is an approximation for *u*, so when (3.6) is substituted into (3.5), the equation will not necessarily equate to zero, i.e.

$$a\frac{\partial^2 \bar{u}}{\partial x^2} + b = e(x) \tag{3.7}$$

where *e(x)* is a non-zero residual.

The weighted residual method requires that the weighted averages of the residual be equal to zero, so

$$\int_{x_1}^{x_2} w_i(x)e(x)dx = 0 \tag{3.8}$$

where $w_i(x)$ is a set of weighting functions.

Theoretically, any set of weighting functions could be selected, and there are several methods used in finite element formulation that use different weighting functions. The most common weighted residual method is the Galerkin method, which equates the weighting function to global *shape functions*. The advantage of the Galerkin method over the other weighted residual methods is that it usually results in symmetrical matrices.

4.1.5 Shape Functions

Consider a one-dimensional heat transfer problem, e.g. radial heat transfer in a long cylinder, subjected to a heat flux of *q*/unit length in the inner surface, and with a fixed temperature of *To* at the outer surface. The exact solution, when the internal heat generation is zero, is

$$T(r) = T_o - \frac{q}{k}\ln\left(\frac{r}{R_2}\right) \tag{3.9}$$

where R_2 is the radius to the outer surface, and k is the thermal conductivity.

Consider a 2 node one-dimensional element with node 1 on the outside face and node 2 on the inside face of the cylinder (fig. 14). Approximate the actual temperature distribution with a linear temperature distribution. The temperature distribution can be given in terms of two linear functions, N_1 and N_2, each of which take the value of unity at the node with which they

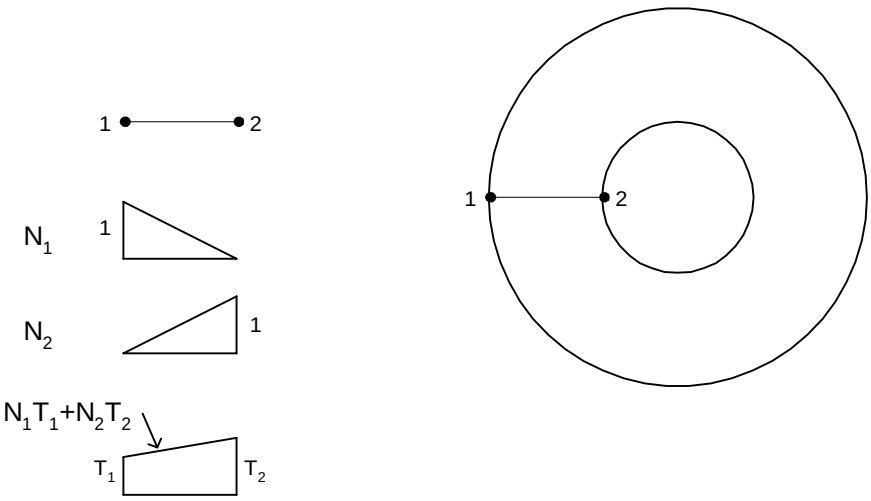

are associated and are zero at the other node.

Figure. 14 One element representation of a one-dimensional finite element model.

A more accurate solution would be found if the radius were divided into three elements and four nodes (fig. 15). Within each element the temperature varies linearly.

Consider a set of approximation functions $N_1(r)$, $N_2(r)$, $N_3(r)$, and $N_4(r)$ associated with each node in the element subdivision. A typical approximation function $N_i(r)$ is zero over the whole mesh, except in the elements connected to node *i*.

At node *i* the function has a value of unity, within the element associated with node *i* the function is linear. These functions are called the *shape functions*.

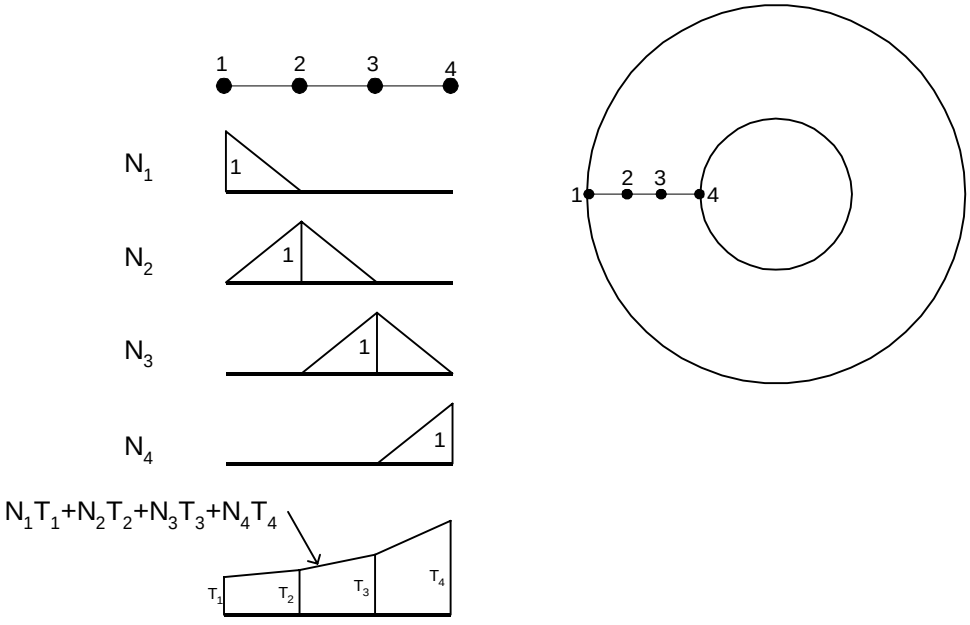

Figure. 15 Three element representation of a one-dimensional finite element model.

It can be seen that the temperature distribution can be represented by the expression

$$T(r) = N_1T_1 + N_2T_2 + N_3T_3 + N_4T_4 \tag{3.10}$$

For an arbitrary number of elements this can be expressed as

$$T(r) = \sum_{i=1}^{n} N_iT_i \tag{3.11}$$

where N_i are the shape functions, and T_i are the nodal temperatures.

Note the similarity of equation (3.11) with equation (3.6).

In the Galerkin form of the weighted residual method, the weighting functions correspond to the shape functions, i.e. $w_i = N_i$ of equation 3.11, or $w_i = \phi_i$ of equation 3.6.

4.1.6 Finite Element Formulation in Two Dimensions

Recall the general form of the two-dimensional steady state heat transfer equation (equation 3.2)

$$k\nabla^2 T + Q = 0 \tag{3.12}$$

or

$$\left(k\frac{\partial^2 T}{\partial x^2} + k\frac{\partial^2 T}{\partial y^2} \right) + Q = 0 \tag{3.13}$$

The method of weighted residuals requires that the weighted averages of the residual be equal to zero

$$\int_A w_i e dA = 0 \tag{3.14}$$

Now, if T is an approximation to the exact temperature distribution, then we can set

$$e = k\frac{\partial^2 T}{\partial x^2} + k\frac{\partial^2 T}{\partial y^2} + Q \tag{3.15}$$

Substituting equation 3.15 into equation 3.14 gives

$$\int_A w_i \left[k\frac{\partial^2 T}{\partial x^2} + k\frac{\partial^2 T}{\partial y^2} + Q \right] dA = 0 \tag{3.16}$$

Green's Theorem states that the integrals of two arbitrary functions ϕ and φ over an area A and its boundary S are related as follows

$$\int_A \left(\frac{\partial \phi}{\partial x}\frac{\partial \varphi}{\partial x} + \phi \frac{\partial^2 \varphi}{\partial x^2} \right) dA = \int_S \phi \frac{\partial \varphi}{\partial x} n_x dS$$

$$\int_A \left(\frac{\partial \phi}{\partial y}\frac{\partial \varphi}{\partial y} + \phi \frac{\partial^2 \varphi}{\partial y^2} \right) dA = \int_S \phi \frac{\partial \varphi}{\partial y} n_y dS$$

Applying Green's Theorem to equation 3.16 results in

$$\int_S \left[k\frac{\partial T}{\partial x} n_x + k\frac{\partial T}{\partial y} n_y \right] w dS - \int_A \left[k\frac{\partial w}{\partial x}\frac{\partial T}{\partial x} + k\frac{\partial w}{\partial y}\frac{\partial T}{\partial y} - Qw \right] dA = 0 \qquad (3.17)$$

Now consider the boundary conditions: the temperature specified over part of the boundary, and the heat flux specified over part of the boundary. At points where the temperature is specified the value of the weighting function is zero. Therefore the first integral in equation 3.17 becomes zero where the temperature is specified. On those parts of the boundary where the heat flux is specified (from equation 3.4c)

$$k\left(\frac{\partial T}{\partial x} n_x + \frac{\partial T}{\partial y} n_y \right) + q = 0$$

or

$$k\left(\frac{\partial T}{\partial x} n_x + \frac{\partial T}{\partial y} n_y \right) = -q \qquad (3.18)$$

Substituting equation 3.18 into equation 3.17 gives

$$\int_S qw dS + \int_A \left[k\frac{\partial w}{\partial x}\frac{\partial T}{\partial x} + k\frac{\partial w}{\partial y}\frac{\partial T}{\partial y} - Qw \right] dA = 0 \qquad (3.19)$$

Recall that the temperature field can be approximated as

$$T = \sum_{i=1}^{n} N_i T_i \qquad (3.20)$$

where N_i are the global shape functions and T_i are the unknown nodal temperatures.

Also note that Galerkin's method sets the weighting function equal to the shape functions

$$w_j = N_j \qquad (3.21)$$

Equation 3.20 and 3.21 are substituted into equation 3.19 to give

$$\int_S qN_j dS + \int_A \left[k\sum_{i=1}^{n} \frac{\partial N_j}{\partial x}\frac{\partial N_i}{\partial x} T_i + k\sum_{i=1}^{n} \frac{\partial N_j}{\partial y}\frac{\partial N_i}{\partial y} T_i - QN_j \right] dA = 0$$

This can be rearranged to give

$$\int_A \left[k \sum_{i=1}^{n} \frac{\partial N_j}{\partial x} \frac{\partial N_i}{\partial x} T_i + k \sum_{i=1}^{n} \frac{\partial N_j}{\partial y} \frac{\partial N_i}{\partial y} T_i \right] dA = \int_A Q N_j dA - \int_S q N_j dS$$

The order of summation and integration can be interchanged

$$\sum_{i=1}^{n} \left[\int_A k \left(\frac{\partial N_i}{\partial x} \frac{\partial N_j}{\partial x} + \frac{\partial N_i}{\partial y} \frac{\partial N_j}{\partial y} \right) dA \right] T_i = \int_A Q N_j dA - \int_S q N_j dS$$

This represents a series of n equations, which may be written in matrix form as:

$$[K]\{a\}=\{f\}$$

[K] is the global "stiffness" matrix, also called the conductivity matrix. *{f}* is the "force vector". The components of these matrices are:

$$K_{ij} = \int_A k \left[\frac{\partial N_i}{\partial x} \frac{\partial N_j}{\partial x} + \frac{\partial N_i}{\partial y} \frac{\partial N_j}{\partial y} \right] dA \qquad (3.22)$$

$$f_i = \int_A Q N_i dA - \int_S q N_i dS \qquad (3.23)$$

In practice, these matrices are established for each element separately, and then assembled to give the global matrices. The global matrices can then be solved for the nodal temperatures by any numerical solution technique.

To show how the element conductivity matrices are derived in practice, the matrices for two types of elements used in SAFIR will be derived in the following section.

4.1.7 Triangular (3 node) Elements

Consider a triangular element, shown in figure 16. The element has three nodes. Each node has one degree of freedom, corresponding to the temperature at the node.

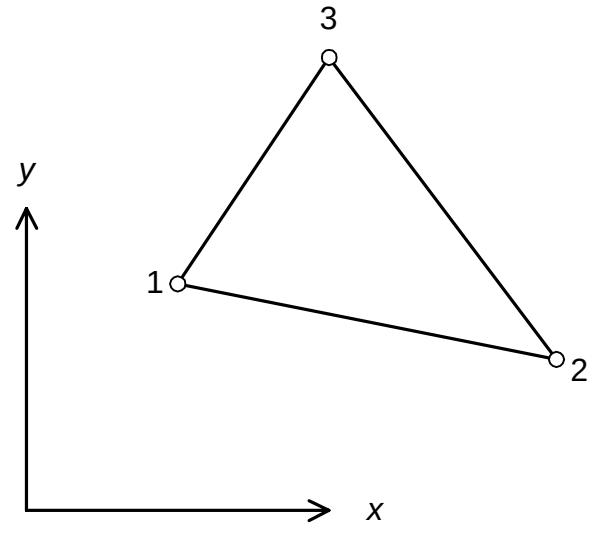

Figure. 16. Triangular finite element.

As the temperature distribution within the element is linear, an expression for the temperature at any point within the element in terms of the x and y coordinates of that point can be written:

$$T = a + bx + cy \tag{3.24}$$

where a, b, and c are constants. If the known temperatures at the nodes are T_1, T_2, and T_3 then the values of the constants a, b, and c can be found by substituting the known nodal temperatures into equation 3.24:

$$\begin{aligned} T_1 &= a + bx_1 + cy_1 \\ T_2 &= a + bx_2 + cy_2 \\ T_3 &= a + bx_3 + cy_3 \end{aligned} \tag{3.25}$$

where x_i and y_i are the coordinates of node i.

Solving equation 3.25 for a, b, and c and substituting into equation 3.24 gives

$$T = \frac{1}{2A}\left[(\alpha_1 + \beta_1 x + \gamma_1 y)T_1 + (\alpha_2 + \beta_2 x + \gamma_2 y)T_2 + (\alpha_3 + \beta_3 x + \gamma_3 y)T_3\right] \tag{3.26}$$

where A is the area of the element, given by

$$A = \frac{1}{2} Det \begin{vmatrix} 1 & x_1 & y_1 \\ 1 & x_2 & y_2 \\ 1 & x_3 & y_3 \end{vmatrix}$$

or

$$A = \frac{1}{2}\left(x_1 y_2 + x_2 y_3 + x_3 y_1 - x_1 y_3 - x_2 y_1 - x_3 y_2\right)$$

and

$$\alpha_1 = x_2 y_3 - x_3 y_2$$

$$\beta_1 = y_2 - y_3$$

$$\gamma_1 = x_3 - x_2$$

with the other components given by cyclic permutation of the subscripts.

The shape functions can be written as

$$N_i = \frac{1}{2A}\left(\alpha_i + \beta_i x + \gamma_i y\right) \tag{3.27}$$

This function is linear, and can be shown to have a value of unity at the node to which it relates and zero at the other nodes. These are the criteria required for the shape function. The profile of a shape function is shown in figure 17.

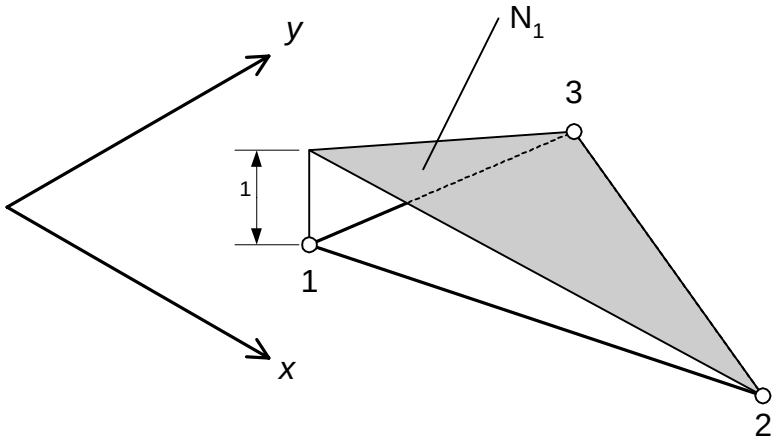

Figure. 17. Typical shape function for a triangular element.

Equation 3.26 can then be written as

$$T = \sum_{i=1}^{3} N_i T_i \tag{3.28}$$

The stiffness matrix for the triangular element can be found by substituting equation 3.27 into equation 3.22, giving

$$K_{ij} = \int_A \frac{k}{4A^2}\left(\beta_i \beta_j + \gamma_i \gamma_j\right) dA$$

If *k* is temperature dependent (which is the case in SAFIR), it is not possible to calculate the stiffness matrix analytically and it has to be done by a numerical technique of integration. The stiffness matrix is symmetric.

(3.29)

The force vector is given by equation 3.23.

The first term in equation 3.23 can be written as

$$\{f\}_Q = Q\int_A \begin{bmatrix} N_1 \\ N_2 \\ N_3 \end{bmatrix} dA \tag{3.32}$$

which results in

$$\{f\}_Q = \begin{bmatrix} QA/3 \\ QA/3 \\ QA/3 \end{bmatrix} \tag{3.33}$$

The second integral of equation 3.23 depends on which side of the triangular element is subjected to the boundary condition. If side 1-2 is subject to the boundary condition then

$$\{f\}_{q,12} = -\int_{S_{12}} qN_i dS = -q\int_{S_{12}} \begin{bmatrix} N_1 \\ N_2 \\ 0 \end{bmatrix} dS \tag{3.34}$$

where S_{12} denotes integration along side 1-2 of the element. The zero term in the matrix arises because N_3 is zero along side 1-2. Substituting L_i for N_i in equation 3.34 results in

$$\{f\}_{q,12} = \frac{-qS_{12}}{2} \begin{bmatrix} 1 \\ 1 \\ 0 \end{bmatrix} \tag{3.35}$$

Similarly

$$\{f\}_{q,23} = \frac{-qS_{23}}{2} \begin{bmatrix} 0 \\ 1 \\ 1 \end{bmatrix}$$

$$\{f\}_{q,31} = \frac{-qS_{31}}{2} \begin{bmatrix} 1 \\ 0 \\ 1 \end{bmatrix}$$

Then the nodal force vector *i*

$$\{f\} = \{f\}_Q + \{f\}_{q,12} + \{f\}_{q,23} + \{f\}_{q,31}$$

4.1.8 Rectangular (4 node) Element

Consider a rectangular element with 4 nodes, see figure 18. In addition to the global coordinate system *x,y,* there is a normalised coordinate system ξ,η with its origin at the centre of the element. Note that, although Figure 0.6 is drawn for a rectangular element with the edges parallel to the global system of coordinates, SAFIR can accommodate any shape

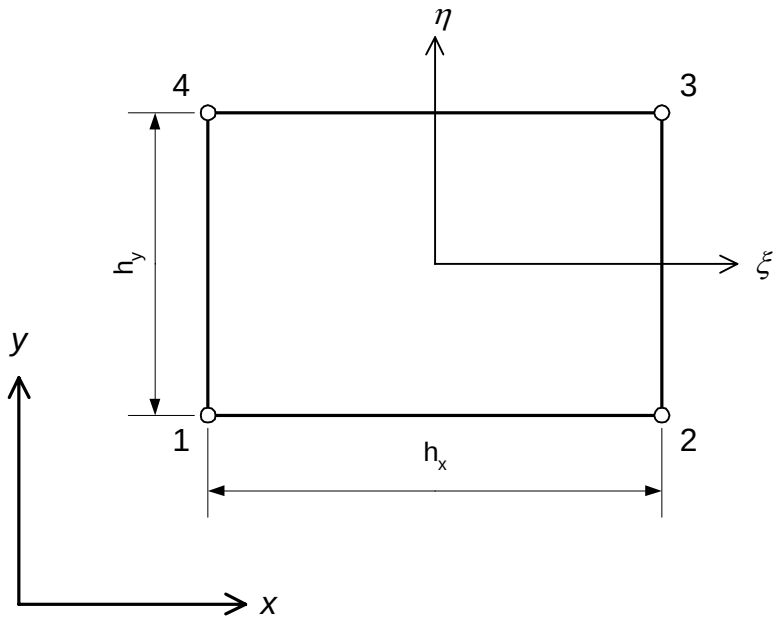

of quadrilateral elements, even irregular ones.

Figure. 18. Rectangular element and normalised coordinate system.

The shape functions for this element are written in terms of the normalised coordinates:

$$\begin{aligned} N_1 &= (1-\xi)(1-\eta)/4 \\ N_2 &= (1+\xi)(1-\eta)/4 \\ N_3 &= (1+\xi)(1+\eta)/4 \\ N_4 &= (1-\xi)(1+\eta)/4 \end{aligned} \qquad (3.38)$$

A shape function for the rectangular element is shown in figure 19.

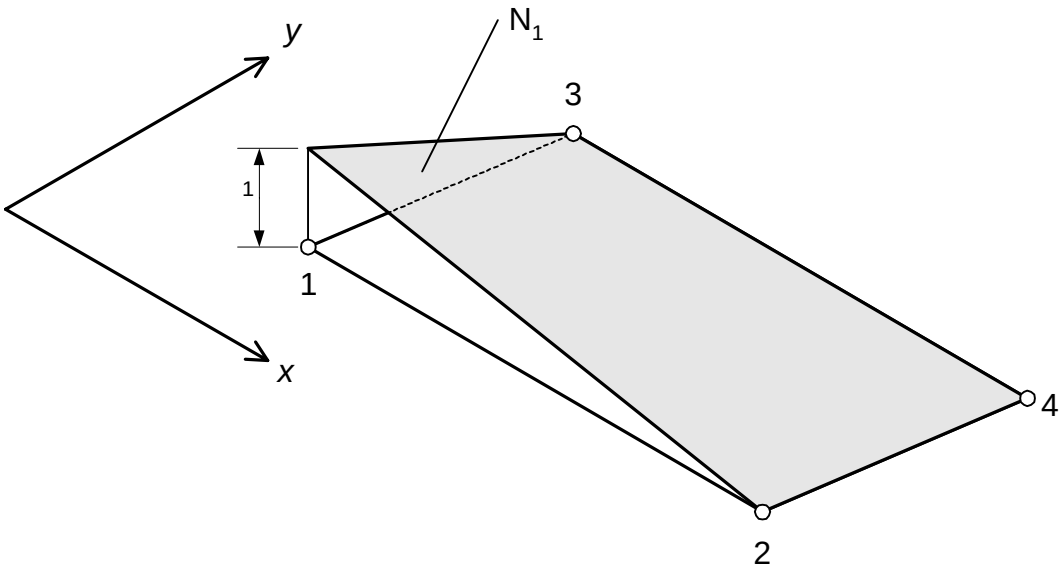

Figure. 19. A typical rectangular element shape function.

All matrices and vector derivations follow the same principles as for the triangular element.

4.1.9 Convective Boundary Conditions

The derivation of the finite element formulation in Section 0 ignored convective heat transfer at the boundaries. To account for convection requires a modification of the basic formulation already developed. Convection is described quantitatively by Newton's Law of Cooling:

$$q = h\left(T_s - T_\infty\right)$$

where q is the convective heat transfer rate per unit area of surface, h is the heat transfer coefficient, T_s is the surface temperature of the body, and T_∞ is the ambient temperature of surrounding medium.

Equation 3.18 then becomes

$$k\left(\frac{\partial T}{\partial x}n_x + \frac{\partial T}{\partial y}n_y\right) = -\left(q + h\left(T - T_\infty\right)\right)$$

Substituting this into equation 3.17 yields

$$\int_S qw + h\left(T - T_\infty\right)dS + \int_A \left[k\frac{\partial w}{\partial x}\frac{\partial T}{\partial x} + k\frac{\partial w}{\partial y}\frac{\partial T}{\partial y} - Qw\right]dA = 0$$

Using equations 3.20 and 3.21 and rearranging gives

$$\sum_{i=1}^{n}\left[\int_A k\left(\frac{\partial N_i}{\partial x}\frac{\partial N_j}{\partial x}+\frac{\partial N_i}{\partial y}\frac{\partial N_j}{\partial y}\right)dA\right]T_i+\sum_{i=1}^{n}\left[\int_S hN_iN_j dS\right]T_i=\int_A QN_j dA-\int_S qN_j dS+\int_S hT_\infty N_j dS$$

this can be expressed in matrix form as

$$([K]+[H])\{a\}=f$$

4.1.10 Time-Dependant (Transient) Problems

Many real problems are time-dependant. The finite element formulation of a transient problem is a relatively simple extension of the steady-state formulation. In addition to specified boundary conditions, transient problems require an initial condition (at time $t = 0$) to be specified.

The transient heat conduction problem is given by equation 3.1b

$$k\nabla^2 T+Q=\rho c\frac{\partial T}{\partial t}$$

The procedure is similar to the steady-state problem. Using a weighted residual method and integrating by parts gives

$$\int_S qwdS+\int_A\left[k\frac{\partial w}{\partial x}\frac{\partial T}{\partial x}+k\frac{\partial w}{\partial y}\frac{\partial T}{\partial y}-Qw\right]dA+\int_A w\left(\rho c\frac{\partial T}{\partial t}\right)dA=0 \qquad (3.46)$$

The weighting function w is not a function of time. A finite element formulation is substituted for *T*, assuming that the time dependence can be separated from the spatial dependence

$$T=\sum_{i=1}^{n}N_i(x)T_i(t) \qquad (3.47)$$

The weighting functions are equated to the shape functions (Galerkin's Method). Equation 3.47 is substituted into equation 3.46, and manipulated as before

$$\sum_{i=1}^{n}\int_A \rho cN_iN_j dA\frac{dT}{dt}+\sum_{i=1}^{n}\left[\int_A k\left(\frac{\partial N_i}{\partial x}\frac{\partial N_j}{\partial x}+\frac{\partial N_i}{\partial y}\frac{\partial N_j}{\partial y}\right)dA\right]T_i=\int_A QN_j dA-\int_S qN_j dS$$

This can be written in matrix form as

$$[M]\{\dot{T}\}+[K]\{T\}=\{Q\}+\{q\} \qquad (3.48)$$

where $M_{ij}=\int_A \rho cN_iN_j dxdy$

and the other terms are unchanged from the steady state formulation.

It is not possible to integrate the equations with respect to time analytically. So they are discretised in time by normal finite element techniques, i.e.

$$\{T\} = \sum N_n(t) T_n$$

If the temperature at the node changes from Tn to Tn+1 over a time interval Δt, then the shape functions are given by (see figure 20)

$$N_n = 1 - \xi$$
$$N_{n+1} = \xi$$

where η varies from 0 to 1 and is given by

$$\xi = \frac{t}{\Delta t}$$

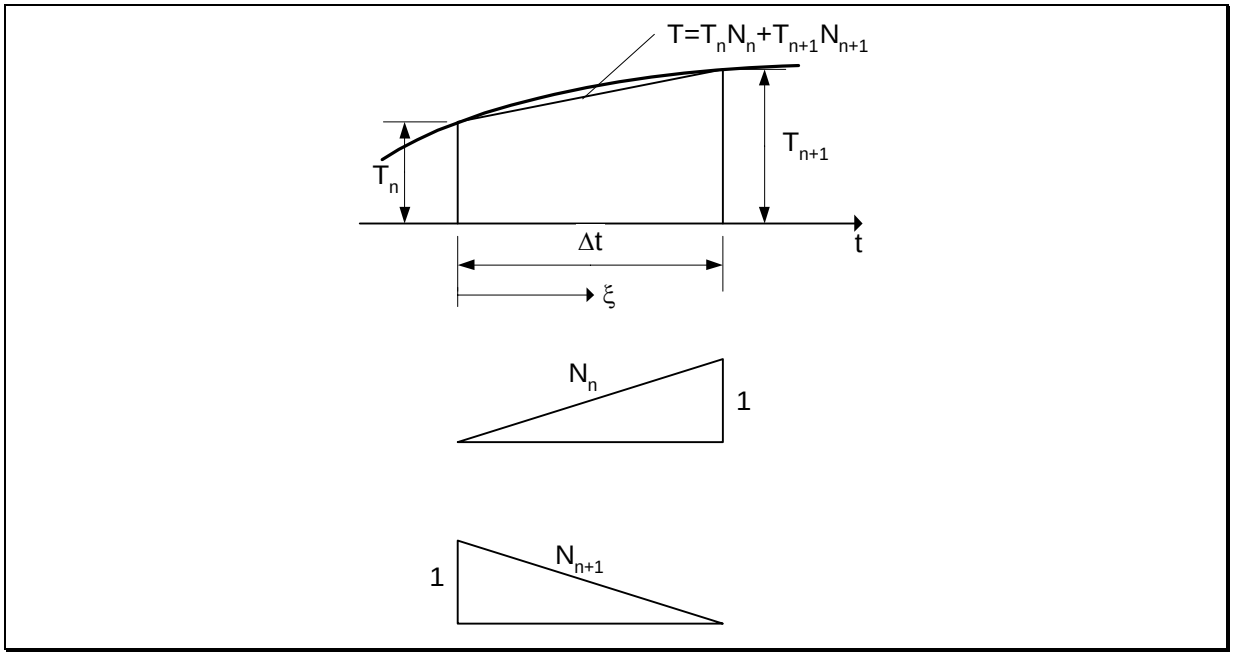

Figure. 20. Temporal shape functions

The derivatives of the shape functions with respect to time are

$$\dot{N}_n = \frac{-1}{\Delta t}$$
$$\dot{N}_{n+1} = \frac{1}{\Delta t}$$

Discretisation of equation 3.48 gives

$$[M]\left\{T_k \dot{N}_k + T_k \dot{N}_{k+1}\right\} + [K]\{T_k N_k + T_{k+1} N_k\} = \{f\} \qquad (3.49)$$

Substituting the expressions for the shape functions and their derivatives into equation 3.49 gives

$$\left(\frac{[M]}{\Delta t}+[K]\theta\right)\{T\}_{k+1}=\left(\frac{[M]}{\Delta t}-[K](1-\theta)\right)\{T\}_k+\{f\} \qquad (3.50)$$

where

$$\theta=\frac{\int_0^1 W_j\xi d\xi}{\int_0^1 W_j d\xi}$$

Equation 3.50 is solved at each time step for the nodal temperatures at time *tk=(k+1)Δt.*

Selection of different distributions for the weighting function, *Wj*, result in different values for θ, as shown in figure 21.

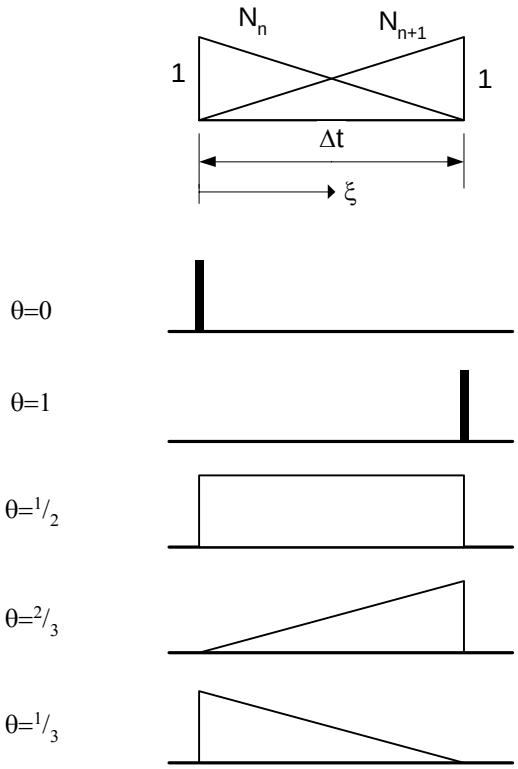

Figure. 21. Weighting functions.

It can be shown that any scheme with θ > 0.5 is unconditionally stable. If θ < 0.5, then the scheme is stable subject to the condition

$$\Delta t \le \frac{2}{(1-2\theta)\lambda_{\max}}$$

where λ_{max} is the maximum eigenvalue of equation 3.48.

Although it is not unconditionally stable, the advantage of the forward difference scheme (θ = 0) is that it is explicit and computationally simple. Other schemes are implicit and require the solution of an equation system at each time step.

TASEF uses θ = 0. SAFIR allows the user to select the value of θ to be used (the parameter TETA in the DAT input file), and recommends a value of 0.9. Zienkiewicz reports that oscillations sometimes occur with θ=½, and for a simple problem involving 10 quadratic elements to model transient heating of a bar it was found values of 2/3 and 0.878 gave improved results.

4.1.11 Non-Linear Problems

Non-linear problems arise when *k,* ρ*,* and *c* are a function of the temperature. The matrix formulation is identical to equation 3.48, except an iterative solution is required at each time step. The simplest iterative method involves starting with an initial guess, T_0, obtaining a more accurate solution be solving the equation

$$[M]\{\dot{T}\}_1 + [K(\{T\}_0)]\{T\}_1 = \{Q\}_0 + \{q\}_0$$

and then repeating the iteration scheme

$$[M]\{\dot{T}\}_n + [K(\{T\}_{n-1})]\{T\}_n = \{Q\}_{n-1} + \{q\}_{n-1}$$

until convergence lies within a suitable tolerance.

4.1.12 Enthalpy formulation

The non-linear problem involves 2 sets of equations. With slightly modified notations, these are:

For the residue, which governs the solution to be obtained,

$$\{r\} = [K]\{T_\theta\} + [C]\frac{\{T_\theta\} - \{T_n\}}{\theta\,\Delta t} - \{g\}$$

For the tangent matrix, which governs convergence towards the solution

$$\left[\frac{\partial\{r\}}{\partial\{T\}}\right] = [K] + \frac{[C]}{\theta\,\Delta t} - \left[\frac{\partial\{g\}}{\partial\{T\}}\right]$$

The capacity formulation amounts to evaluate the capacity matrix [C] at time t_θ and to use this value directly in both equations. This can lead to problems if the capacity exhibits sharp variations with temperature.

Figure 1 shows the case when the temperature within a time step increases from T_i to T_{i+1}. T_θ is the temperature evaluated during the iterations, at time t_θ. The first iteration is noted **a**, whereas the second iteration is noted **b**.

With a capacity formulation, see the upper part of the Figure, the capacity may change dramatically from a to b, which can create convergence problems and, even more problematic, can lead to converging towards a solution that is missing totally the energy contained in the peak if the time step is too long. This will be the case if solution b is considered as a converged solution.

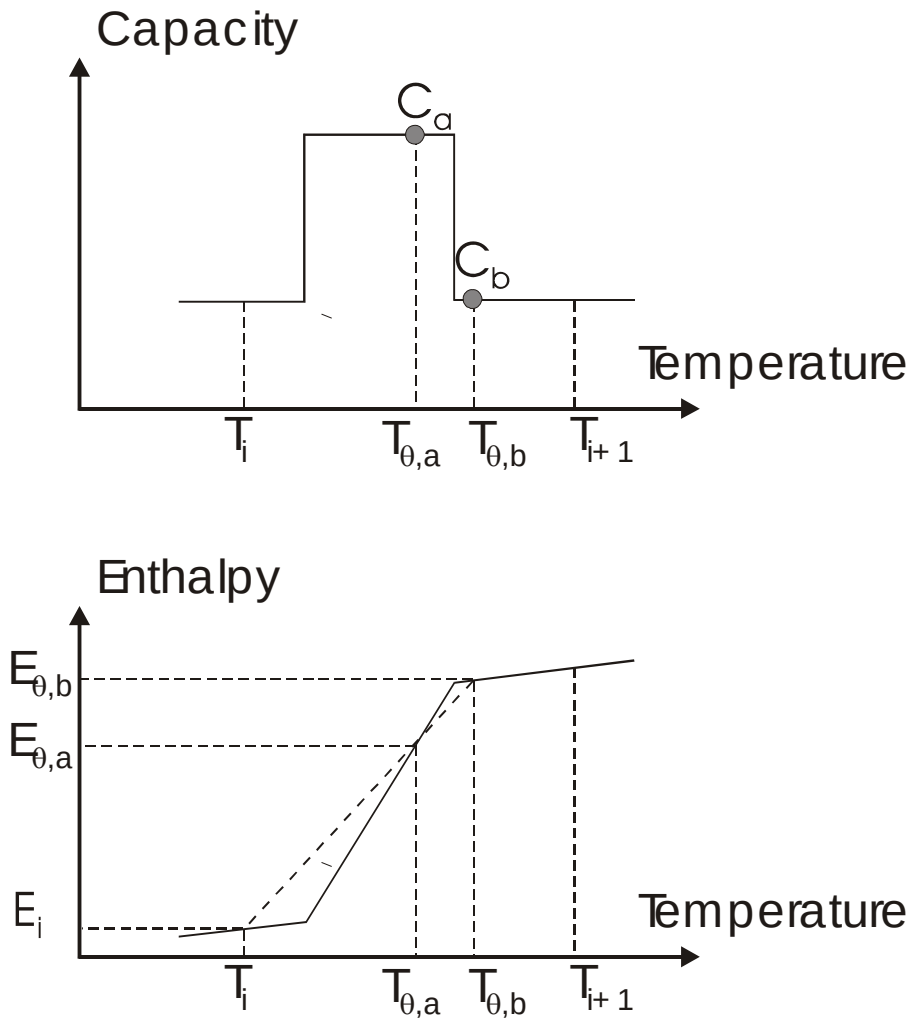

Figure 1 : Capacity versus Enthalpy formulation

The other possibility is to evaluate the enthalpy according to

$$E(T) = \int_0^T C(u)\,du$$

and the capacity to be used in the iteration process according to

$$C = \frac{E(T_\theta) - E(T_i)}{T_\theta - T_i}$$

In fact, this amounts to evaluate the average value of the capacity from T_i to T_θ. In the lower part of the Figure, this average capacity is indicated by the slope of the line from $(T_i;E_i)$ to (T_θ,E_θ).

The graph shows that the enthalpy curve is more continuous than the capacity curve and thus, the iteration matrix is less disturbed by slight variations of the temperature during the iteration process (in the Figure, the slope happens to be exactly the same for iterations **a** and **b**). Convergence is thus improved in the sense that less iterations are generally required for a given time step.

More important is the fact that the value of the energy contained in the peak is not missed, even if no temperature is encountered in the peak during the iteration process. Convergence of the solution to the "exact" solution as a function of the size of the time steps is thus also improved, which means that bigger time steps can be used.

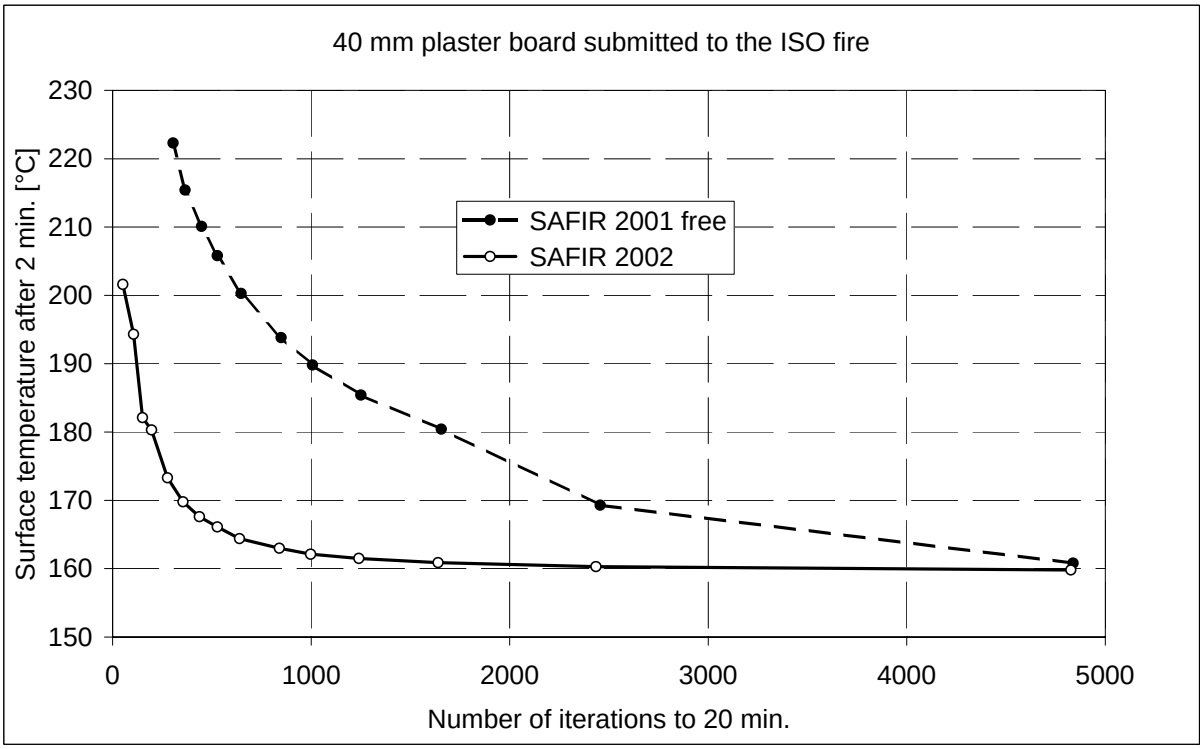

Figure 2 : comparison of the convergence

This is exemplified in Figure 2. It shows the evolution of the temperature on the surface of a 40 mm plaster board (discretised by ten 4 mm finite elements) exposed to 2 minutes of ISO fire as a function of the number of iterations that are required to simulate 20 minutes of fire. The curve noted "SAFIR 2001 free" has been calculated with a capacity formulation whereas the curve noted "SAFIR 2002" has been calculated with an enthalpy formulation. The highest number of iterations is obtained with a time step of 1 seconds, then 2, 3, 4, 5, 8, 10, 12, 15, 20 and, for the enthalpy formulation only, with 30, 60 and 120 seconds.

The first advantage mentioned previously is very marginal; nearly the same number of iterations is required in both formulations for a given time step. It has yet to be mentioned

that convergence was obtained by the enthalpy formulation with very long time steps that did not allow convergence by the capacity formulation.

The second advantage is clearly visible here; a "precision" of 10°C was obtained with 7 times less iterations (2456/355), and a precision of 1°C with 3 times less iterations (4838/1639).

Practically speaking, if the specific heat **c** and the specific mass ρ are known at 2 temperatures T_0 and T_1 with $T \in [T_0,T_1]$, with a linear variation assumed for both properties, then the enthalpy at temperature T is calculated according to

$$
\begin{aligned}
E(T) &= \int_0^T C(u)\,du \\
&= \int_0^{T_0} C(u)\,du + \int_{T_0}^T C(u)\,du \\
&= E(T_0) + \int_{T_0}^T C(u)\,du \\
&= E(T_0) + \int_{T_0}^T \left[c_0 + \frac{c_1 - c_0}{T_1 - T_0}(u - T_0) \right] \left[\rho_0 + \frac{\rho_1 - \rho_0}{T_1 - T_0}(u - T_0) \right] du \\
&= E(T_0) + \int_{T_0}^T [k + l\,u]\ [m + n\,u]\,du \\
&= E(T_0) + k\,m(T - T_0) + (l\,m + k\,n)\left(\frac{T^2 - {T_0}^2}{2} \right) + l\,n\left(\frac{T^3 - {T_0}^3}{3} \right)
\end{aligned}
$$

with

$$
\begin{aligned}
l &= \frac{c_1 - c_0}{T_1 - T_0} \\
k &= c_0 - l\,T_0 \\
n &= \frac{\rho_1 - \rho_0}{T_1 - T_0} \\
m &= \rho_0 - n\,T_0
\end{aligned}
$$

4.2 Internal voids

For thermal calculations in 2-D situations, the structure can have internal voids filled with air, as in hollow core concrete slabs, or H-steel sections encased in a box of thermally insulating material.

Each void is surrounded by NFR frontier elements. As far as linear elements are concerned, each element E_i has the two nodes: N_i and N_{i+1}. Each N_i node belongs to two elements : E_{i-1} and E_i.

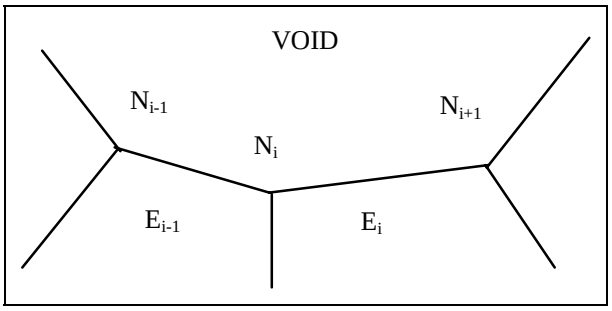

Figure 12: Void frontier

Convection and radiation are treated separately.

4.2.1 Convection

The hypothesis is that the specific heat of the air is so small that it is neglected. Then, at any time, the fictitious temperature of the air in the void is uniform, determined by the convective fluxes received from all the elements:

$$\oint_L q_c \, dL = 0 \ \text{[W/m]}$$

with q_c : convective heat flux [W/m²]
L : length of the frontier surrounding the void [m]

With the FE formulation, we have a linear convective flux:

$$\sum_{i=1}^{NFR}\left(\sum_{n=1}^{nip} h_n \, \omega_n \, hE_i \left(T_v - T_n\right) LE_i\right) = 0 \ \text{[W/m]},$$

or, in the particular case of linear elements,

$$\sum_{i=1}^{NFR} \frac{LEi}{2} hE_i \left(T_v - TN_i + T_v - TN_{i-1}\right) = 0 \ \text{[W/m]},$$

where n: point of integration
nip: number of integration points on the frontier of an element

h_n: value of the shape function at point n
ω_n: weight at point n
hE_I: convection factor of the material in element E_i
T_v: fictitious temperature of the air in the void
T_n: temperature at point i
LE_i: length of the frontier of the element E_i
TN_i: temperature at node I

The last equation can be written as:

$$T_v \sum_{i=1}^{NFR} LE_i\ hE_i \;=\; \sum_{i=1}^{NFR} \frac{LEi}{2} hE_i \left(TN_i + TN_{i-1}\right) \;=\; \sum_{i=1}^{NFR} TN_i\ LN_i \text{ [W/m],}$$

where $LN_i \;=\; \dfrac{hE_{i-1}\ LE_{i-1} + hE_i\ LE_i}{2}$ [W/mK].

It comes:

$$T_v \;=\; \frac{\sum_{i=1}^{NFR} TN_i\ LN_i}{\sum_{i=1}^{NFR} LE_i\ hE_i} \;=\; \frac{\sum_{i=1}^{NFR} TN_i\ LN_i}{\sum_{i=1}^{NFR} LN_i} \text{ [K].}$$

The convective heat flux at each node is then given by:

$$gN_i \;=\; LN_i \times \left(T_v - TN_i\right) \text{ [W/m].} \qquad (8)$$

The derivative of the flux, used in the iteration matrix, is given by:

$$gN_{i,j} \;=\; LN_i \times T_{v,j} \;=\; \frac{LN_i\ LN_j}{\sum_{t=1}^{NFR} LN_t} \text{ [W/mK].} \qquad (9)$$

This matrix is symmetric. This contribution (Equation 9) to the matrix of iteration has not been programmed in SAFIR because it would dramatically increase the bandwidth of the problem. It is perfectly possible to reach the correct equilibrium state, provided Equation 8 is correctly considered, even with an approximate matrix of iteration.

4.2.2 Radiation

The physical phenomena on each frontier element are radiation, illumination and net heat flux going out of the surface. They are defined by the following equations:

$$R_i \;=\; \varepsilon i\,\sigma\,T_i^4 + \rho i\ H_i \;=\; \varepsilon i\,\sigma\,T_i^4 + \left(1-\varepsilon i\right) H_i \text{ [W/m²]}$$

$$H_i \;=\; F_{ij}\ R_j \text{ [W/m²]}$$

$$q_i \;=\; \varepsilon i\,\sigma\,T_i^4 - \alpha i\ H_i \;=\; \varepsilon i\,\sigma\,T_i^4 - \varepsilon i\ H_i \text{ [W/m²]}$$

5 *Convergence Criteria*

Fint	Internal forces. Those forces are calculated at the nodes as the result of the internal forces coming from the elements: axial forces, bending forces
$du^{i,j}$	incremental displacement at time step i and iteration j
NDOF	Number of Degrees Of Freedom of the structure
NE	Norm of the Energy, calculated at each iteration
NET	Norm of the Total Energy, calculated as the summation of all the previous NE
PRECISION	a number, chosen by the user, supposed to be small

At the beginning of the program:

NET = 0

At each iteration of each time step:

$$NE = \sum_{k=1}^{NDOF} \left| du_k^{i,j} \; F\,\mathrm{int}_k \right| \qquad (10)$$

NET = NET + NE
IF (j ≤ 1) THEN
CRITER = 1
ELSE
IF (NET = 0) THEN
CRITER = 0
ELSE
CRITER = NE / NET
ENDIF
ENDIF
IF (CRITER < PRECISION) then
convergence has been obtained
ELSE
convergence has not been obtained
ENDIF

Note that NE is neither exactly the energy nor the norm of the energy. It has the dimension of an energy because forces multiply displacements. This has the advantage of giving equal importance to displacement-force type variables and to moment-rotation type variables. The relative importance of these two groups of variables is also not dependent on the unit, which has been chosen for length, (metre or mm, for example) or for force (Newton or KiloNewton, for example). It is not exactly the energy because a force associated to a negative displacement should be counted as a negative energy, whereas it is counted as positive in Equation 10. Each component of Equation 10 is counted as positive because, if not, the negative components would tend to reduce the energy NE, and if by chance the sum of the negative components is exactly equal to the sum of the positive components, this would give NE = 0, whereas the iteration under consideration has produced a lot of incremental movements. Even if all displacements and forces are positive, NET is not exactly the energy, as can be seen on the next figure, drawn for a system with 1 D.o.F., a load applied in two time steps under constant temperature TO, and then the temperature changing from T0 to T1 in one time step.

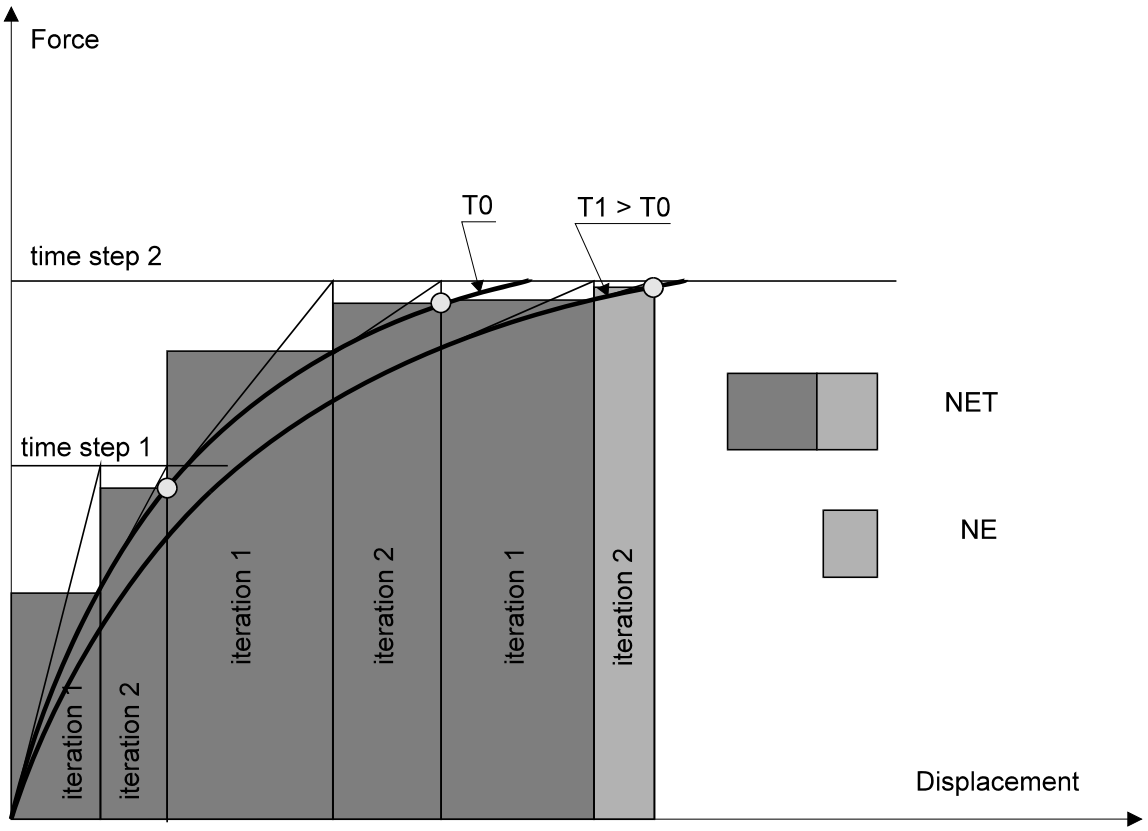

Figure 13: Convergence iterations

6 *Storage of Stiffness Matrix*

The stiffness matrix is supposed to be symmetric. Only the upper part is stored.

The matrix K is divided in 3 parts K11, K12=K21 and K22

$$\underline{\underline{K}} = \begin{bmatrix} K11 & K12 \\ K21 & K22 \end{bmatrix} \qquad (11)$$

Index 1 is related to the undefined D.o.F., where the solution has to be calculated.
Index 2 is related to the fixed D.o.F., where the solution is prescribed.
Many of the K11 elements have the value 0, it is stored by the *skyline* technique.
Matrix K11 is stored in the REAL vector RIGE.

An INTEGER vector, NSTSKY is associated to the vector RIGE to retrieve the position of K11(i,j) in RIGE.
NSTKY(j) is the position of K11(j,j) in RIGE.
The retrieving function is IFCTSKY(i,j,NSTSKY). It calculates the position of K11(i,j) in RIGE:
IFCTSKY(i,j,NSTSKY) = NSTSKY(j)+i-j with $i \leq j$

Example:

If matrix K11 has the following non 0 elements, they are stored in RIGE in the order 1, 2, 3.

K1 =

1	2		6					
	3	4	7					
		5	8					
			9	10		13		
				11		14		
					12	15	17	
						16	18	
							19	

RIGE = { K11(1,1) ; K11(1,2) ; K112,2) ; K11(2,3) ; K11(3,3) ; K11(1,4) ; K11(2,4) ,K11(3,4) ; ..... }

NSTSKY = { 1 ; 3 ; 5 ; 9 ; 11 ; 12 ;16; 19 }

For example:
K11(3,4) is stored in RIGE(IFCTSKY(3,4,NSTSKY) = RIGE(NSTSKY(4)+3-4) =
RIGE(9+3-4) = RIGE(8)

NUACTIFS is the dimension of K11 and NSTSKY
ILARGEUR11 is the dimension of RIGE

The K12 part is stored in rK12, although it is stored in the manner of K21
K12(i,j) is stored in rK12(j-NUACTIFS,i) with i.le.j

7 NOMENCLATURE

E = Young's modulus
lp = Limit of proportionality
e = Exponent of the law
D = Factor of the law
S = Stress
fy = Yield strength of steel
fc = Compressive strength of concrete
ft = tensile strength of concrete
 = Strain
 = Stress

8 REFERENCES

1 Franssen, J.M. "Étude du Comportement au Feu des Structures Mixtes Acier-beton". Thèse de Doctorat en Sciences Appliquées, No. 111, Université de Liège, Belgium, 1987.

2 Schleich, J.B. "REFAO-CAFIR: Computer Assisted Analysis of the Fire Resistance of Steel and Composite Concrete-steel Structures". CEC Research 7210-SA/502, Final Report EUR 10828 EN, Luxembourg, 1987.

3 Schneider, U. "Behaviour of Concrete at High Temperatures". Rilem-Committee, 44-PHT, 1983.

4 Franssen, J.-M. "Contributions a la Modelisation des Incendies dans les Bâtiments et de leurs Effets sur les Structures", Université de Liège, Belgium, 1998.

4 Mason, J. E. "Heat Transfer Programs for the Design of Structures Exposed to Fire", Univ. of Canterbury, Christchurch, 1999.

5 Reddy J.N. and Gartling, D.K. 1994. The Finite Element Method in Heat Transfer and Fluid Dynamics. CRC Press.

6 Zienkiewicz O.C. and Taylor R.L. 1989. The Finite Element Method. McGraw-Hill. London.

7 Lewis R.W., Morgan K., Thomas H.R., Seetharamu K.N. 1996. The Finite Element Method in Heat Transfer Analysis. John Wiley & Sons. England.